A Bio-Physically Inspired Silicon Neuron

Ethan Farquhar, *Student Member, IEEE,* and Paul Hasler, *Senior Member, IEEE*

Abstract—The physical principles governing ion flow in biological neurons share interesting similarities to electron flow through the channels of MOSFET transistors. Here, is described a circuit which exploits the similarities better than previous approaches to build an elegant circuit with electrical properties similar to real biological neurons. A two-channel model is discussed including sodium (Na^+) and potassium (K^+). The Na^+ channel uses four transistors and two capacitors. The K^+ channel uses two transistors and one capacitor. One more capacitor simulates the neuron membrane capacitance yielding a total circuit of four capacitors and six transistors. This circuit operates in real-time, is fabricated on standard CMOS processes, runs in subthreshold, and has a power supply similar to that of real biology. Voltage and current responses of this circuit correspond well with biology in terms of shape, magnitude, and time.

Index Terms—Analog circuits, bioelectric potentials, biological cells, nervous system.

THE discussion in this paper describes what we believe is a very new way of looking at the electrical properties of biological neurons. Much work has been accomplished in the field of neuroscience since the early 1950's with the pioneering work of Hodgkin and Huxley [1]. Advances have also been made in the field of semiconductors, however, little of our understanding of the physics of semiconductors has carried across to models of ion flow in biology. Here, we show a model of a two-channel type [sodium (Na^+) and potassium (K^+)] neuron circuit which is capable of generating action potentials, and elegantly accomplishes this with just six transistors.

Fig. 1 shows two parallel views for understanding and modeling ion flow in biology. Both views start from the biological action potential. Underlying the action potential is ion flow through channels. From this point the two views begin to diverge. The classical view (left path) seeks to model the system by empirically deriving equations describing the current through a population of channels. While these equations do capture many of the important dynamics present in channels, they are not physically based. That is, they are not derived from a set of fundamental forces underlying the ionic motion. They are, instead, curve fit approximations to data that was taken. As is the case with any equations that are not directly tied to physical properties, they are difficult to implement in the real world, and frequently lead to large, convoluted circuits.

In contrast to the above approach, we sought to use the numerous similarities between biological channels and semiconductor channels to develop a circuit which behaves as a neuron
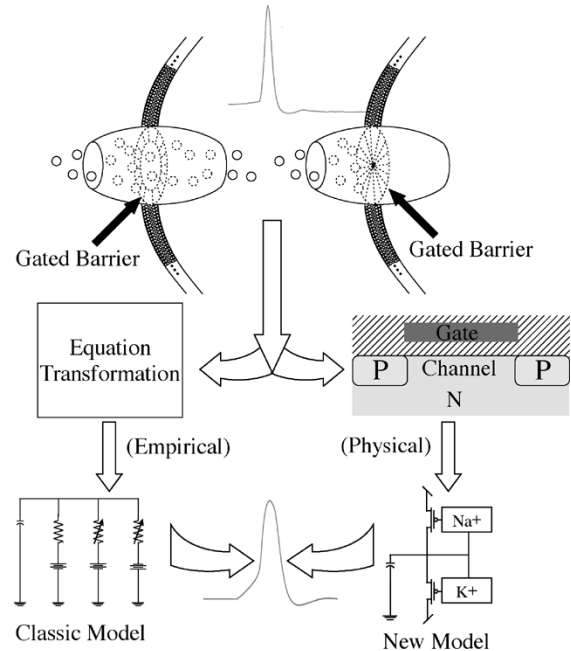
Fig. 1. Two parallel views for modeling electrical activity in neurons. The path down the left side describes the classical path taken by neuroscientists. The right shows the path that we have chosen, and shows the progression from bio-physics to the corresponding silicon physics. Both views start with an action potential (in this case from the particular snail *helisoma trivolvis*). Both views also acknowledge the ionic currents and their underlying macro-transport phenomenon. However, the classical view seeks to extrapolate equations from the data and develop a model of the system based off of these equations. This, we term the empirical method. The other method requires one to look at the numerous direct analogies between biological channels and MOSFET transistor channels. We believe this leads to a totally new way of looking at the biology. Both methods can lead us to an action potential, however, the path on the right not only gives results consistent with biological data, but also can be directly realized.

does (right path). The remainder of this document seeks to develop further the reasoning and method behind the development of this circuit and the path down the right side of Fig. 1. We start with a description of the underlying biological mechanisms to compare them with the corresponding transistor ones.

I. BIOLOGICAL PRIMER

In 1952, Hodgkin and Huxley described the electrical activity of squid axons in a series of papers that eventually won them the Nobel Prize in 1963 [1]. They showed that two types of channels are essential to generate an action potential (neuronal voltage response), and they developed an electrical model to describe them. This model (shown in Fig. 2) has become the cannonical circuit model, but it has one large fault for the circuit designer. It lacks the ability to be directly realized physically due to the fact that the variable resistor (or conductance) given by g_{Na} and g_K
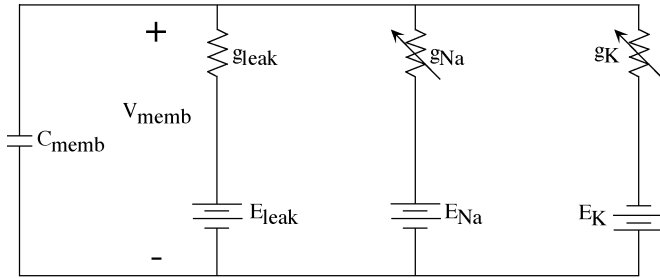
Fig. 2. Original circuit model of neural electrical conductivity as devised by Hodgkin and Huxley. This circuit looks simple, but hidden in the details is a very complex model for the variable conductances.

requires an unknown circuit element. Note that the authors concede that physical implementations of the Hodgkin and Huxley model do exist in which the designer has *implemented* the equations, however no one has every built the circuit shown in Fig. 2. Let us quickly review how these channels operate, in the next three subsections.

A. Neuron Physics

Neurons are the active part of a nervous system. They are electrically excitable and conductive. These cells have a semi-permeable membrane which separates many different charge carriers; the charge separation qualities of the membrane are nicely modeled by a simple capacitor labeled C_{mem} in Fig. 2. All charge is carried by electrically charged ions, that is, molecules which have either gained or lost an electron from their valence shell. There are many different ions that affect neural activity, but for the purpose of this discussion, we will focus only on Na^+ ions and K^+ ions as Hodgkin and Huxley showed that these are the only two required for action potential generation. Both ions carry a $+1$ charge.

These electrically charged ions are available in certain limited concentrations both inside and outside the cell. Na^+ has a high concentration outside with respect to the inside, and K^+ has a high concentration inside the cell with respect to the outside. The channels do not have a mechanical means of forcing ions across the membrane (neglecting such things as the $\mathrm{Na}^+ \setminus \mathrm{K}^+$ pump which does not figure into this discussion). Instead, ion flow is governed by two fundamental forces: drift and diffusion. Diffusion (the primary current) and drift currents are in opposition to each other. The batteries in Fig. 2 indicate at what point they are equal. This point, known as the reversal or Nernst potential, is calculated using the Nernst equation

$$E_x = \frac{RT}{F} \ln \frac{[C_x]_o}{[C_x]_i} \qquad (1)$$

with $[C_x]_o$ and $[C_x]_i$ being the outside or inside concentrations of the ions respectively. (RT/F) is equal to the thermal voltage $((kT/q)$ or 25.8 mV) and is hereafter termed U_T. Using this equation $E_{\mathrm{K}} \approx -70$ mV and $E_{\mathrm{Na}} \approx 55$ mV. These values assume the use of ion concentrations for the squid that Hodgkin and Huxley used. These numbers will vary for different animals with different concentrations.

At rest the cell sits at a voltage termed V_{rest}. This voltage is also related to the concentration of particular ions both inside and outside the cell, and the relative permeability of the cell
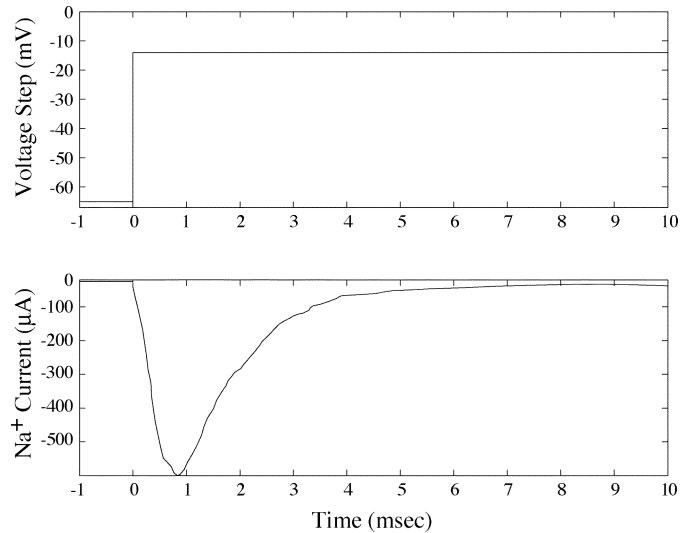

Fig. 3. Upper plot shows the voltage step forced across the membrane during a voltage clamp experiment. Lower plot shows the current through the Na^+ channel (step response) [1].

to that ion. Specifically, V_{rest} is defined by the Goldman–Katz equation

$$V_{\mathrm{rest}} = U_T \ln \frac{P_{\mathrm{K}}[\mathrm{K}^+]_o + P_{\mathrm{Na}}[\mathrm{Na}^+]_o}{P_{\mathrm{K}}[\mathrm{K}^+]_i + P_{\mathrm{Na}}[\mathrm{Na}^+]_i} \qquad (2)$$

where P_x is the permeability of the respective ion. When evaluated, this equation yields a resting voltage near -60 mV. Values for calculations of (1), (2) from [2].

B. Na$^+$ Channel

Using the above facts, Hodgkin and Huxley developed a series of experimental procedures which enabling them to study the different pieces of the squid neuron. The voltage clamp technique steps the voltage from one voltage to another (step response), and measures the current flowing through the channels. They realized the current they measured was actually the sum of more than one current. Using pharmacological agents, they selectively blocked certain ionic currents, thereby allowing the study of a single type of channel.

The Na^+ channel is one of the two channels essential to generate an action potential. This channel is voltage gated meaning that it responds to changes in voltage across the membrane (V_{mem}). It has both an activating and inactivating mechanism causing current magnitude to increase and then decrease as time progresses. The step response of the Na^+ channel shown in Fig. 3 is derived from their paper [1]. Electrical engineers should recognize this response as that of a bandpass filter, although it has not classically been described as such. The Na^+ channel has two time constants, called τ_m and τ_h for the fast and slow time constants respectively. Data from this channel was curve fit by Hodgkin and Huxley with the following:

Na Equations:

$$I_{\mathrm{Na}} = g_{\mathrm{Na}}(V_m - E_{\mathrm{Na}})$$
$$g_{\mathrm{Na}} = \overline{g_{\mathrm{Na}}} m^3 h$$
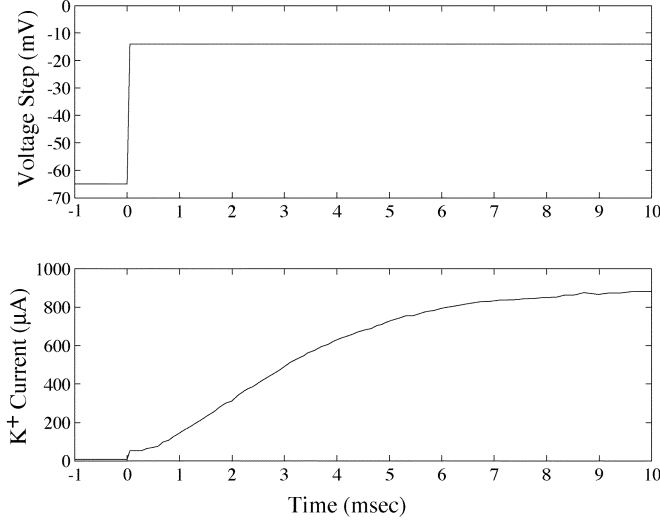$$\frac{dm}{dt} = \alpha_m(1-m) - \beta_m(m)$$

Fig. 4. Upper plot shows the voltage step forced across the membrane during a voltage clamp experiment. Lower plot shows the current through the K^+ channel (step response) [1].

$$\frac{dh}{dt} = \alpha_h(1 - h) - \beta_h(h)$$

$$\alpha_m = \frac{0.1(V_m + 25)}{\left[\exp\frac{V_m+25}{10} - 10\right)}$$

$$\beta_m = 4\exp\left(\frac{V_m}{18}\right)$$

$$\alpha_h = 0.07\exp\left(\frac{V_m}{20}\right)$$

$$\beta_h = \frac{1}{\left(\exp\frac{V_m+30}{10} + 1\right)}. \tag{3}$$

C. K^+ Channel

The K^+ channel is also voltage gated. However, unlike the Na^+ channel, it is only activating. The step response shown in Fig. 4 is also derived from their paper [1]. This has the very characteristic low pass response to a step input. While the time constant is still quite fast, it is clear from comparing Figs. 3 and 4 that the time constant (τ_n) for I_K is much slower than either of the time constants found in I_{Na}. Similar to the Na^+ channel, data was curve fit with the following:

K Equations:

$$I_K = g_K(V_m - E_k)$$

$$g_K = \overline{g_K}n^4$$

$$\frac{dn}{dt} = \alpha_n(1 - n) - \beta_n(n)$$

$$\alpha_n = \frac{0.01(V_m + 10)}{\left[\exp\frac{V_m+10}{10} - 1\right]}$$

$$\beta_n = 0.125\exp\left(\frac{V_m}{80}\right). \tag{4}$$

D. Combined Currents Produce Action Potential

An action potential is the product of many different types of currents interacting with each other. The two previously discussed are the minimum to generate a response, while others
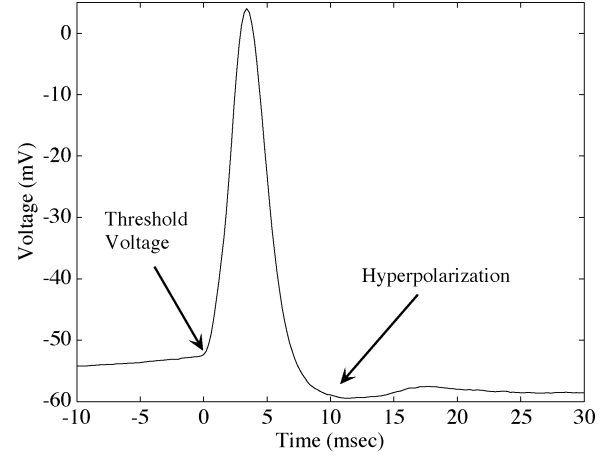

Fig. 5. Real action potential from the invertebrate snail (*helisoma trivolvis*). Note that omitted from this graph is the rise from resting potential to threshold voltage, although threshold can be clearly seen. Also note that Hodgkin and Huxley used a squid for their preparation. The concentrations of the various ions are different in the squid than for this snail. Due to this, various voltages (i.e. V_{rest}, E_{Na}, E_K, etc.) are different, but the theory is the same.

(beyond this paper) modulate it in some way. A typical action potential from the snail *helisoma trivolvis* is shown in Fig. 5.

Spontaneous activity is not found in typical neurons. An outside force acts on the cell (whether it be an input synapse, current injection, or some other mechanical means beyond the scope of this paper) causing the voltage across the cell membrane to rise. If the input is not strong enough to cause the cell to reach to the threshold potential, the cell will simply return to its resting voltage. However, at the threshold voltage (V_{th}), the Na^+ channels open very rapidly allowing Na^+ ions to flow into the cell. This increases the cell's voltage (depolarization) quite quickly. This can be seen in the sharp rise in voltage in Fig. 5. In time, these channels start to close (due to the slower pole)causing the voltage rise to slow down and eventually stop. While the Na^+ channels are closing, the slower responding K^+ channels start to respond and source current out of the cell causing a decrease in cell voltage (re-polarization). The K^+ channel has such a slow time constant it will actually overshoot the desired voltage and hyperpolarize the cell for a period of time.

II. PREVIOUS WORK

Since one can show voltage versus current relationships for these channels, one might be tempted to model these channels as variable conductances. In fact, starting with Hodgkin and Huxley, this is exactly the method that has been employed to date. Hodgkin and Huxley used a variable resistor to model this behavior. The resistor they chose has the dynamics shown in (3), (4) [Fig. 6(b)]. This element, however, is a linearized conductance model of the channel.

Maholwald and Douglas employed a similar technique [4]. They have developed a circuit which is realizable in current technology. However, they seem to have used a very large-scale integration (VLSI) approximation of the linearized conductance that Hodgkin and Huxley postulated. In their paper [4, p. 516], they state that the geometry of the conductance transistor was modulated to make it behave more ohmically than regular devices, indicating the use of a short channel device. Fig. 6(c)
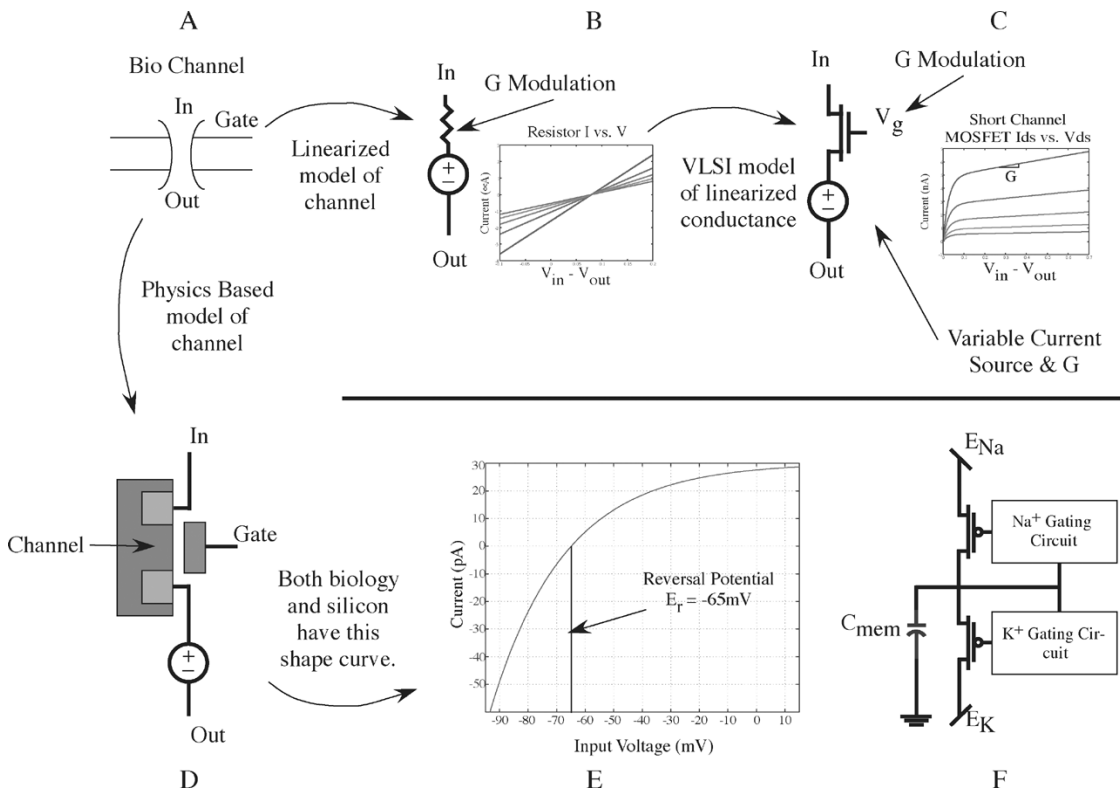
Fig. 6. (a) Hodgkin and Huxley recorded data from ion channels to create their model. (b) Their model utilizes a linearized conductance to model the channel. True, the conductance can be modified, but it is always linear. Note that in their paper [1] it is clear that their model does not fit the data very well. (c) Other VLSI models have relied on their equations (or some other set of equations) and have used VLSI techniques to approximate the linear conductance that Hodgkin and Huxley first proposed. For instance, a short channel length transistor in saturation can be used to approximate this conductance as was done in [4]. (d) In contrast to this is our model which relies on the physical similarities of MOSFETs and ion channels. (e) In a true I–V plot of a channel, one would expect a figure similar to that shown here. For some small operating range, the conductance can be modeled linearly. However, the conductance clearly is not linear. A transistor and ion channel should have this same type of curve since the same macro-transport phenomenon exists in both technologies. (f) This gives rise to a simplified circuit model. The transistor is not a linear model of a conductance, but rather is a model of the channel itself.

clearly shows that such a device can approximate the conductances that Hodgkin and Huxley postulated. The E_{K} and E_{Na} voltages they used clearly put the device into saturation, but the conductance of the transistor can still be tuned by modifying the gate voltage.

Obviously, a control circuit to modulate the gate voltage needed to be developed. For this control, they sought to implement the Hodgkin and Huxley equations. They realized that the rate equations (3) and (4) had the same shape as a tanh curve. A simple diff pair circuit also has a tanh curve, and was therefore used to implement them. The results of this circuit are admirable, but the actual implementation of the equations was not perfect. For example, instead of implementing m^3h as Hodgkin and Huxley specified, they implemented $m - h$. This circuit model also is very large due to the large number of transistors. This does not allow for many of these circuits to be implemented on a reasonably sized chip.

Simoni and Deweerth took this concept further [5]. They added adaptation to their circuit model thereby reducing the sensitivity to mismatch, and they chose a different set of equations to model (see [6]). Adaptation is a large jump in progress as it lends itself to investigation of interesting neural behaviors. However, the basic design procedure of this circuit remains the same as the Maholwald and Douglas case. They used differential pairs to implement the needed curves found in the equations. Again, the results of this work are admirable, but implementing equations leads to large circuits.

Georgiou *et al.* developed another Hodgkin Huxley circuit implementing the equations [10]. The authors uses a subcircuit termed a Bernoulli Cell which is capable of implementing Bernoulli differential equations. They translate the Hodgkin Huxley equations to the form capable of being implemented in a Bernoulli cell, and then plug in the appropriate cell for that equation. Results from the simulated circuit show the concept works, but again, the resulting circuit is quite large.

III. CIRCUIT OVERVIEW

It is our contention that the implementation of equations, particularly the Hodgkin Huxley equations, is not the best method of modeling neurons in VLSI. We have discussed these equations because they are the cannonical set. Others have developed equations which are more correct at predicting actual biological behavior than the Hodgkin and Huxley equations [3]. This shortcoming was noted by Hodgkin himself [7]. It is important to note that equations with variables converted to numbers represent the equations for a specific animal (e.g. Hodgkin and Huxley's equations only describe the squid). The basic physical forces remain the same for every animal while the particulars (concentrations of ions, etc.) are different.

Instead, we believe many similarities between the physics of neurons and the physics of silicon exist. It is the goal here to describe a circuit which makes use of these similarities instead of relying on equation implementation. Certainly differences exist in the physics. As pointed out in [8] one is dealing with ions moving in a fluid (bosons), while the other electrons in substrate (fermions). Due to this difference the MOSFET can only asymptotically approach a slope of (kT/q) per e-fold of current change, while the biology is not limited to this [9, Fig. 4.6]. Our claim is not that the physics are equivalent, but that they are good approximation of each other. Ask yourself, if the MOSFET had been around in 1952, and Hodgkin and Huxley had understood it, would they have used a different circuit model?

Biological channels allow current to flow through a membrane. They have a nonlinear exponential current relationship to the voltage on the membrane. This relationship simply cannot be accomplished using a resistor. One would ideally like to replace them with elements which also have an exponential relationship between voltage and current. This brings to mind two types of devices: a bipola junction transistor (BJT), and a subthreshold MOSFET transistor. We chose to use the MOSFET transistor for several reasons: the extremely low amounts of power dissipated by it in subthreshold, current levels from it are naturally comparable in magnitude to those seen in biology, it is smaller, available in standard CMOS processes, and we don't have to deal with base currents. Fig. 6(b) shows the model as described by Hodgkin and Huxley while Fig. 6(d)–(f) shows our new conception.

As stated before, the primary driving force in ionic channels is diffusion. This same fact is true in a subthreshold MOSFET. This accounts for the exponential I-V relationship. Since the driving force is the same type of force, we have replaced the ionic channel with a silicon channel (the channel of the MOSFET, Fig. 6(d)). Biasing the transistor so that it operates in the ohmic regime [Fig. 6(e)] allows the transistor to naturally operate in a nonlinear regime closely related to biology. The natural range between E_{Na} and E_{K} of ~150 mV naturally biases them in the ohmic regime.

Biological channels are really made up of two high level parts: the pore (the physical structure that ions flow through) and the gating mechanism which controls the opening and closing of the pore. Sub-threshold MOSFETs have this same idea. The channel of the MOSFET is a piece of silicon between the drain and the source (Fig. 1), and the voltage gating mechanism modulates the channel. A MOSFET's gating mechanism comes out to a wire and does not have dynamical control built into it. If one could develop a circuit with same dynamics as the gating mechanisms of the biological channel to be modeled, it could simply be connected to this wire; resulting in the same high level structure being preserved, Fig. 6(f).

The current through ion channels has an exponential I–V relationship if one looks at a population of channels. Current through an individual channel is stochastic. This fact also holds true for MOSFETs. Imagine the existence of a MOSFET of extremely small width (~1 nm). If one could measure the current through the channel it would also be stochastic in nature. If many of these transistors were connected in parallel, the resulting current would be the familiar smooth exponential curves.
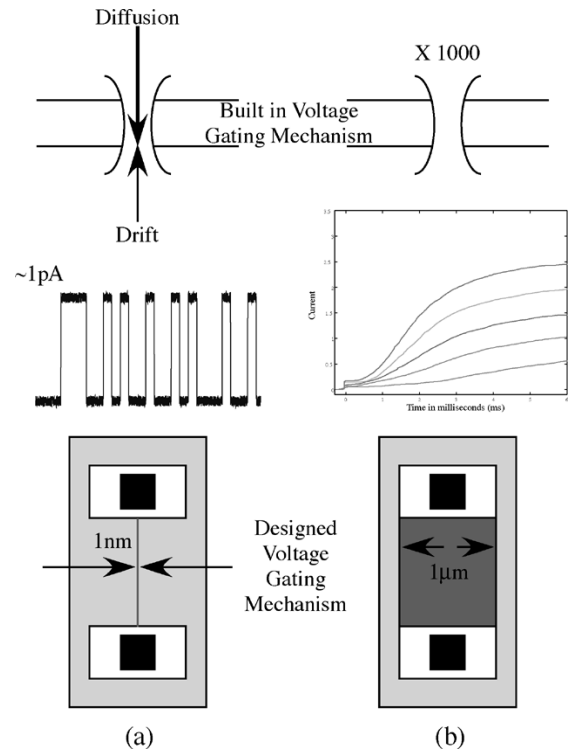

Fig. 7. This discussion of biological channels, modeled by transistors, actually refers to models of channel populations. (a) A single biological channel is stochastic in nature. That is current through it shows a on/off behavior, not the smooth current curves that have been discussed to this point. Smooth currents require a large population of channels to be present. The same phenomenon can be observed with an extremely small width transistor (≈1 nm in width). (b) However, when a transistor of reasonable width is used (as in our case), smooth currents can be generated in much the same way that a large population of biological channels can generate smooth currents.

Obviously, the process is different (bosons versus fermions) between the technologies, but the same stochastic phenomenon is present. Many small parallel MOSFETs are equivalent to a single MOSFET of width equal to the sum of the smaller transistors. Therefore, a MOSFET with reasonable width actually models a population of biological channels, Fig. 7.

A. Na$^+$ Circuit

Having established the use of a MOSFET as an analog to an ion channel, now the design of the control circuitry can be undertaken.

The step response of the biological Na$^+$ channel has already been described as a bandpass filter. Looking at Fig. 8 certain parameters in the design of this circuit become apparent. This figure shows voltage data taken from Hodgkin and Huxley's paper [1] on the x-axis, while the y-axis shows us the voltage needed on the gate of a MOSFET transistor to get the needed current out of it. In other words, take a voltage step on a biological channel and measure the resulting peak current; then relate that value to the voltage needed on the gate of a MOSFET to get an equivalent current flowing through it. It is easy to see several regions of operation in this curve, with the first region showing a definite gain in the system. Since the gain parameter, determined to be ≈8, was so obviously important, any amplifier design had to incorporate this value. This gain parameter aids in overcoming the natural (kt/q) limitation described in [8].
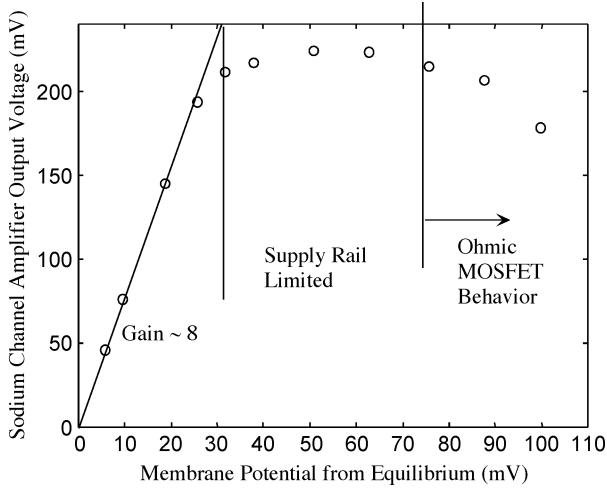
Fig. 8. The Na$^+$ channel has a set of complex dynamics that seem hard to model. However, looking at the step response data shown in Fig. 3, it should become clear that this channel is a bandpass filter. The above plot shows that this channel is also a linear amplifier (with a gain of approximately 8) that saturates, and then eventually rolls off. We know that we get a current out of the channel when we place a voltage across it, and we know that the same is true for a MOSFET. This plot shows the voltage placed across the biological membrane on the x-axis, and the voltage needed on the gate of a transistor to get the same current out of it on the y-axis.

This gain value was the only concrete value which was used in the design of this amplifier. There was a strong desire to make the poles of this circuit adjustable since it is our belief that many different channel types can be modeled by changing this gain term and the pole locations [11]. With that in mind, Fig. 9 shows the Na$^+$ amplifier circuit and the controlled channel transistor. This tunable bandpass filter has poles which can be moved based on voltages placed on the nodes $V_{\tau m}$ and $V_{\tau h}$. This feature will enable the circuit to respond as quickly as the biological circuit does by setting the biases. The following equations are derived to relate the time constants to the currents in the transistors, and the capacitor sizes.

B. Na$^+$ Bias Voltage Calculations

The Na$^+$ circuit shown is a modified bandpass amplifier. Consequently, there are several regions of operation for this particular circuit. Two areas of interest for this application include the low- and high-frequency regions. The really high-frequency region (capacitive feedthrough) is outside the range of operation for this application, although the derivation of its time constant, τ_{cap}, is shown as it naturally flows from the other derivations.

1) Low-Frequency Model: To find the low-frequency corner, an important assumption is made. Assume that the current through M_{τ_h} is large enough to keep up with any changes to V_{mem}. Therefore, the voltage V_g is held constant.

Start with the following node equation:

$$(C_{\text{Na}} + C_Z)\frac{dV_g}{dt} = C_{\text{Na}}\frac{dV_{\text{mem}}}{dt} + C_Z\frac{dV_{\text{Na}}}{dt}$$
$$+ I_{\tau_h} e^{\frac{(-\kappa \Delta V_{\tau_h})}{U_T}} \left[e^{\frac{\Delta V_{\text{Na}}}{U_T}} - e^{\frac{\Delta V_g}{U_T}} \right]. \quad (5)$$

However, V_{τ_h} does not change (as it is a fixed voltage) and V_g is being held constant. As a result, the above equation simplifies to

$$C_Z \frac{dV_{\text{Na}}}{dt} = -C_{\text{Na}} \frac{dV_{\text{mem}}}{dt} - I_{\tau_h} \left[e^{\frac{\Delta V_{\text{Na}}}{U_T}} - 1 \right]. \quad (6)$$

Next, define a new term $X = e^{-\Delta V_{\text{Na}}/U_T}$ and $(dX/dt) = -e^{-\Delta V_{\text{Na}}/U_T}(\Delta V_{\text{Na}}/U_T)$ and plug these into the above equation to get:

$$\frac{C_Z U_T}{I_{\tau_h}} \frac{dX}{dt} = -\frac{C_{\text{Na}} X}{I_{\tau_h}} \frac{dV_{\text{mem}}}{dt} + (X - 1) \quad (7)$$

The low-frequency cutoff (τ_h) is defined by

$$\tau_h = \frac{C_Z U_T}{I_{\tau_h}}. \quad (8)$$

Note that the subscript h does not refer to the word "high," but rather to the h term used by Hodgkin and Huxley actually making it the low-frequency pole.

2) High-Frequency Model: To solve for the high-frequency corner, again an assumption must be made. Assume the capacitive currents are much greater than the currents flowing through the feedback transistor (M_{τ_h}). The following equation results:

$$(C_{\text{Na}} + C_Z)\frac{dV_g}{dt} = C_Z \frac{dV_{\text{Na}}}{dt} + C_{\text{Na}}\frac{dV_{\text{mem}}}{dt}. \quad (9)$$

At extremely high frequencies, the currents through the transistors are negligible as compared with the currents through the capacitors. Thus a capacitive feed-through regime will eventually be observed with the following equations holding:

$$\frac{\Delta V_g}{\Delta V_{\text{mem}}} = \frac{C_{\text{Na}}(C_Z + C_{\text{leak}})}{(C_{\text{Na}} + C_Z)(C_Z + C_{\text{leak}}) - C_Z^2} \quad (10)$$

$$\frac{\Delta V_{\text{Na}}}{\Delta V_{\text{mem}}} = \frac{C_{\text{Na}} C_Z}{(C_{\text{Na}} + C_Z)(C_Z + C_{\text{leak}}) - C_Z^2}. \quad (11)$$

However, what happens between the low-frequency cutoff and the capacitive feedthrough regime? A composite circuit combing traits of the low-frequency and high-frequency circuit results. This circuit has an initial jump (for voltage step) due to capacitive feedthrough which is counteracted by the pseudo-floating-gate voltage (V_g). This voltage settles back to equilibrium due to current through the feedback transistor (M_{τ_h}). To derive this equation the equation for the low-frequency model is combined with the high-frequency model resulting in the following equation:

$$(C_Z + C_{\text{leak}})\frac{dV_{\text{Na}}}{dt} + I_{\tau_m} e^{\frac{(-\kappa \Delta V_g)}{U_T}} = C_Z \frac{dV_{\text{mem}}}{dt}. \quad (12)$$

After substitution

$$\frac{(C_Z + C_{\text{leak}})(C_{\text{Na}} + C_Z) - C_Z^2}{C_Z I_{\tau_m}} \frac{dV_g}{dt} -$$
$$\frac{C_{\text{Na}}(C_Z + C_{\text{leak}})}{C_Z I_{\tau_m}} \frac{dV_{\text{mem}}}{dt} = e^{\frac{(-\kappa \Delta V_g)}{U_t}} - 1. \quad (13)$$

Once again a variable substitution is utilized with $Y = e^{(\kappa \Delta V_g)/U_T}$ and $(dY/dt) = e^{(\kappa \Delta V_g)/U_T}(\kappa \Delta V_g/U_T)$. This yields the following:

$$\tau_m \frac{dY}{dt} = \frac{\kappa \tau_{\text{cap}}}{U_T} Y \frac{dV_{\text{mem}}}{dt} + 1 - Y \quad (14)$$

where $\tau_{\text{cap}} = C_{\text{Na}}(C_Z + C_{\text{leak}})U_T/C_Z I_{\tau_m}\kappa$ which denotes the starting point of capacitive feedthrough and
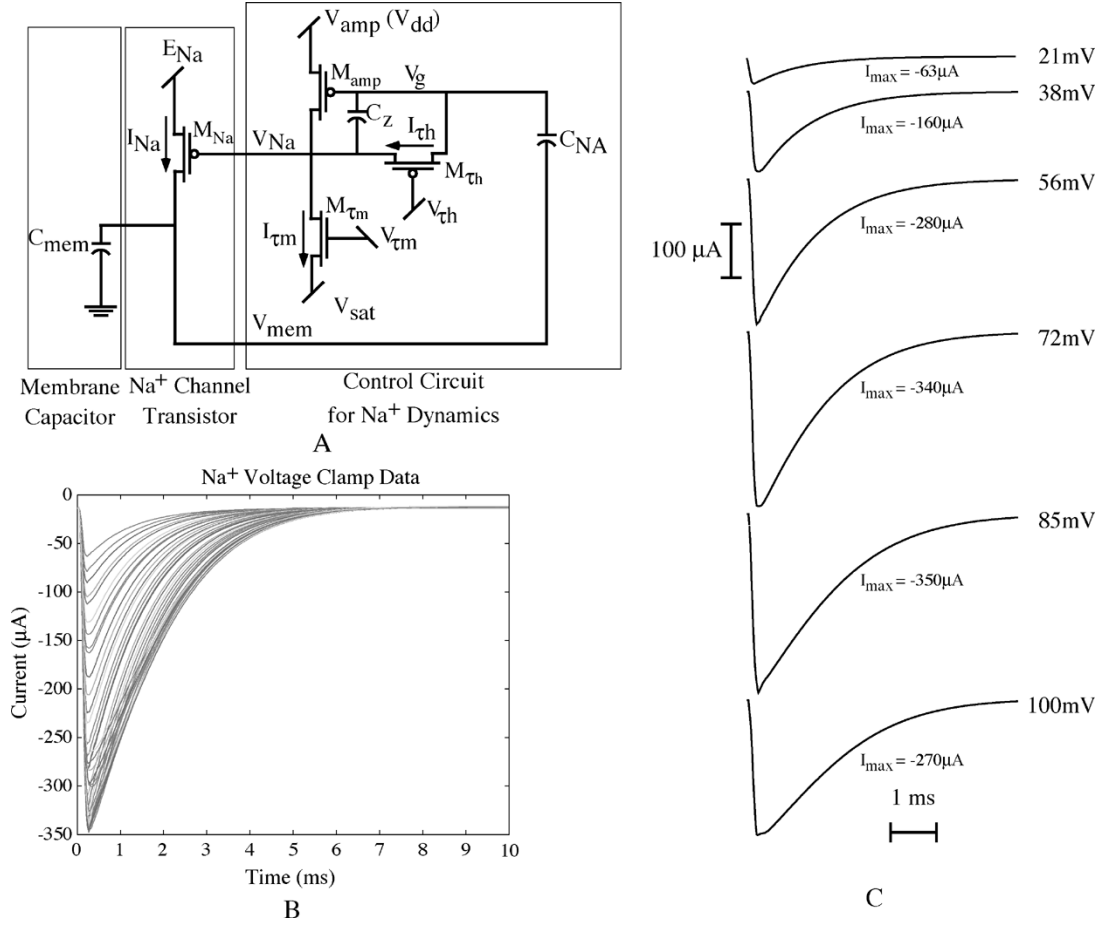
Fig. 9. (a) The Na$^+$ circuit. One can easily see the channel transistor and membrane capacitor. Connected to the channel transistor is the circuit which controls its dynamics. It is a bandpass filter with a gain term (set by the relationship between $C_{\rm Na}$ and C_z). (b) Data from the Na$^+$ voltage clamp experiments performed in lab. These responses are indicative of the bandpass filter that was implemented. Notice that as the input voltage approaches $E_{\rm Na}$ the max current decreases and starts to approach 0 again. Although, not shown here, when the input step voltage exceeds $E_{\rm Na}$, the current will start to flow in the opposite direction, as one would expect. (c) Selected data from (b) for clarity.

$\tau_m = ((C_Z + C_{\rm leak})(C_{\rm Na} + C_Z) - C_Z^2)/C_Z I_{\tau_m}(U_T/\kappa)$ is the high-frequency cutoff time constant of interest. This neuron circuit should never run at frequencies that would place it in the capacitive feedthrough regime.

The gain for this circuit can be shown to be $A_{\rm Na} = C_{\rm Na}/C_Z$. From the previously mentioned data (Fig. 8), this value needs to be ~8. The capacitors are chosen by this ratio.

Step response data from this circuit is shown in Fig. 9. Select data from the left is blown up on the right for clarity. This data shows resulting currents for input steps up to 100 mV. The current magnitude increases as expected until the input step approaches $E_{\rm Na}$ (the reversal potential) at which point the magnitude starts to decrease, as can be seen in the data.

C. K$^+$ Circuit

Similar to the terms τ_m and τ_h, Hodgkin and Huxley used the term τ_n. This term described the time constant of the activation of the K$^+$ channel. A similarly named V_{τ_n}, is the bias controlling the activation time constant of the K$^+$ channel. In other words, it controls where τ_n is. The following equation gives the equation for current through this transistor:

$$I = I_o e^{\frac{(\kappa V_{\tau n})}{U_T}}\left(e^{\frac{-V_{gk}}{U_T}} - e^{\frac{-V_{\rm K}}{U_T}} \right). \tag{15}$$

The conductance of this transistor at any given value of V_{sd} can be found by taking the partial derivative of the current with respect to V_{sd}. In our case, V_{sd} is $V_{\rm K}$ This yields

$$\frac{\partial I}{\partial V_{\rm K}} = I_o e^{\frac{(\kappa V_{\tau n})}{U_T}}\left(e^{\frac{-V_{\rm K}}{U_T}} \times \frac{1}{U_T} \right). \tag{16}$$

At steady state, since the voltage V_{gk} and $V_{\rm K}$ equal each other, we know that the difference between the source and drain voltage (V_{sd}) is 0. So, if we plug this into the above equation we get

$$\frac{\partial I}{\partial V_{\rm K}} = I_o e^{\frac{(\kappa V_{\tau n})}{U_T}} \frac{1}{U_T}. \tag{17}$$

We rename $I_o e^{(\kappa V_{\tau n})/U_T}$ to $I_{\rm sat}$ because this is the same equation for a subthreshold transistor that is in saturation. We know that the time constant of a node is equal to the resistance seen at that node times the capacitance seen there (or RC). Therefore with $\partial I/\partial V_{\rm K} = g_k = 1/R_k$, we multiply $R_k C_k$ and get the following:

$$\frac{\partial I}{\partial V_{\rm K}} = I_{\rm sat}\frac{1}{U_T} = \frac{1}{R_k}$$

$$R_k C_k = \frac{U_T C_k}{I_{\rm sat}} = \tau_n$$
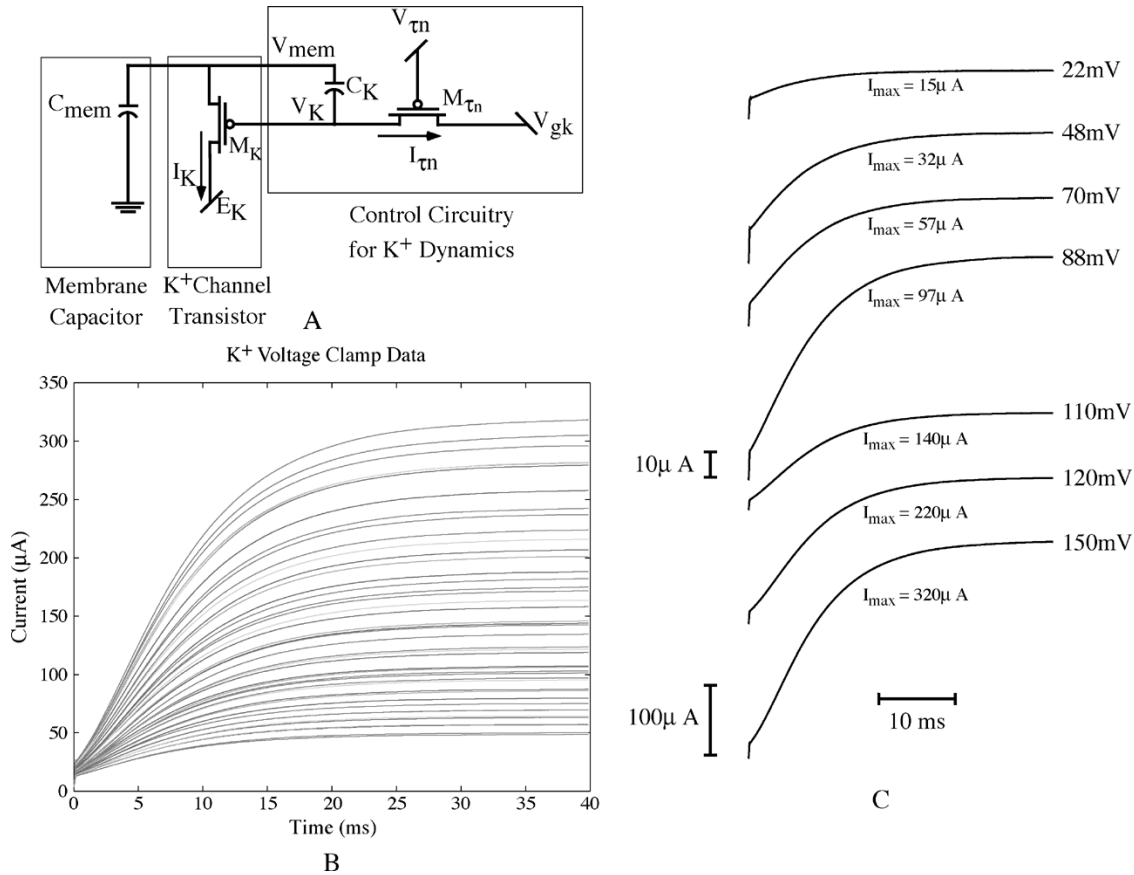
$$I_{\rm sat} = \frac{U_T C_k}{\tau_n}$$

Fig. 10. (a) The K$^+$ circuit. Again, it is easy to see the channel transistor and the membrane capacitor. The circuit connected to the channel transistor is a low-pass filter, as is needed from observing the step response for a biological channel shown in Fig. 4. (b) Data from the K$^+$ voltage clamp experiments performed in the lab. Note that all show a low pass response. Note also an instantaneous jump in current at onset. In our circuit this is due to capacitive coupling from V_{mem} to V_{K}. This is expected, and if one closely examines Hodgkin and Huxley's data, this same step is apparent, and therefore desirable. (c) Selected data from (c) for clarity.

However, the substituted current I_{sat} is actually the desired current and is therefore renamed I_{τ_n}. Thus, the following equation:

$$I_{\tau_n} = \frac{U_T C_k}{\tau_n}. \qquad (18)$$

Knowing the needed time constant for this node determines the amount of current needed given a particular capacitor size. Using Hodgkin and Huxley's data it was determined that this time constant should be in the neighborhood of 5 ms. At steady state, the nodes V_k and V_{gk} are the same value so 0 current will flow through this transistor. An input step causes a difference between the two nodes causing current to flow. Most input steps do not cause a depolarization enough to put the transistor in saturation, with different step sizes causing different conductances. This means that the time constant for this low-pass filter will be slower for smaller input steps and faster for larger ones. This correlates to what Hodgkin and Huxley actually measured, and is therefore desirable. The use of this transistor also makes the conductance in the channel nonlinear. This helps to preserve the "S-shaped" curve seen in Fig. 4.

Voltage step data is shown for this circuit in Fig. 10. Select data from the left is blown up on the right for clarity. Notice the step in current at the onset of the pulse. This is due to the capacitive coupling from V_{mem} to V_{K}. This phenomenon was desirable, as the same step can be seen in Hodgkin and Huxley's

Fig. 11. The maximum currents reached for both I_{Na} and I_{K} under voltage clamp conditions. Notice the reversal in sign for the Na$^+$ channel. This is due to the input step being larger than E_{Na}. Results are consistent with biology. This is experimental data.

data. Note also that the current magnitude keeps increasing as the voltage step keeps increasing. This is due to the fact that E_{K} is below the resting voltage so the input steps never cross it. These voltage clamp experiments (performed on the Na$^+$ and K$^+$ channels) were meant to emulate those done by Hodgkin and Huxley.
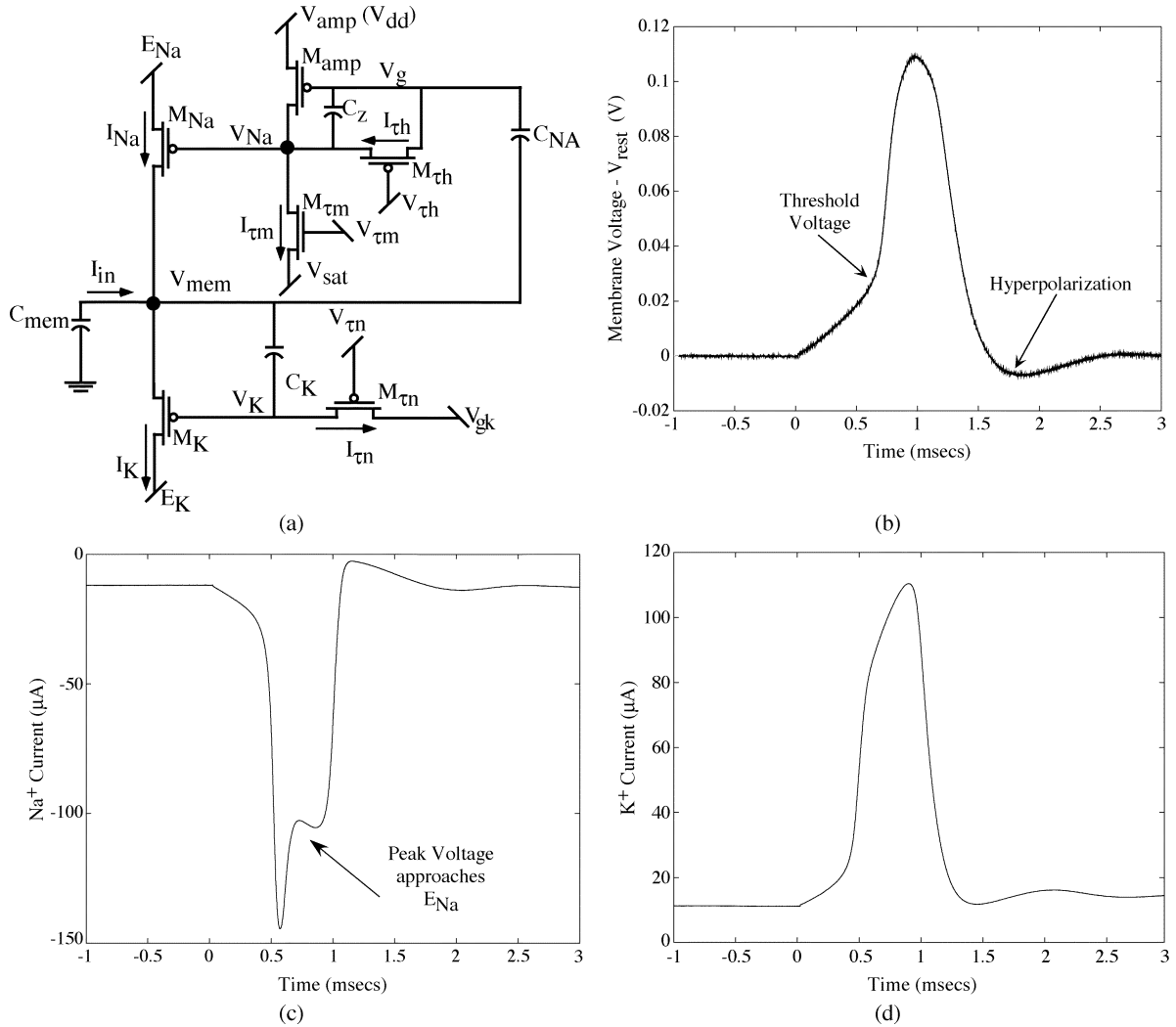
Fig. 12. (a) Complete neuron model circuit as a combination of Na$^+$ and K$^+$ transistor channels. Notice that in terms of size, it is roughly that of an AND gate. (b) Action potential generated by the circuit. Due to the tunability of the circuit, there can be significant variation in shape from one action potential under a certain set of bias conditions to the next. However, within a fixed set of biases, the action potentials all look alike regardless of the input current magnitude (obviously within the boundary conditions of the circuit). The voltage shows the voltage of the spike minus the voltage of the circuit at rest. This was done to show the relative pulse size of an action potential from this circuit. (c) Current through the Na$^+$ channel during an action potential. Notice the kink as time approaches 1 msec. Notice that in Fig. 12(b) that the action potential is at its peak around 1 msec. This peak is very close to the reversal potential for Na$^+$, and therefore causes the current magnitude to decrease (less driving force). This can also be seen in biological Na$^+$ channels. (d) The current in the K$^+$ channel during an action potential. Its shape also models the biology. All three of these plots show experimental data from the same action potential.

The maximum currents reached for each input voltage step is shown in Fig. 11. This clearly illustrates that as the input step increases, I_{Na} also increases to a point. But as the input step gets close to E_{Na} the maximum starts to decrease, to the point where it actually changes direction. E_K is below the input step so it never turns around. The shape of both of these curves is consistent with biology, [12, Fig. 6.3].

D. Neuron Circuit

The spiking neuron is created by tying these two circuits together. Much like the biology, the interplay between the two currents on the membrane node yields the desired behavior. Tying these circuits together gives us another point to consider, the resting voltage V_{rest}. A resting voltage where nothing will ever happen can be observed. This is expected, and is tied to the steady state conductance of each of the channel transistors.

In one case, the K$^+$ conductance is too high causing V_{mem} to sit at some low voltage ($\sim E_K$). The K$^+$ circuit easily sinks any current the Na$^+$ circuit may try to source, thus keeping the charge on C_{mem} steady. The resting current through the K$^+$ transistor can be tuned by the V_{gk} node. At dc, the gate on M_K will equal the voltage V_{gk}. By moving V_{gk}, the steady state conductance of M_K can be brought into balance.

In the second case, the Na$^+$ conductance is too high causing V_{mem} to move to a high voltage ($\sim E_{Na}$). The Na$^+$ circuit can source much more current than K$^+$ channel can sink. This is an equally undesirable case, as no action potentials can be created. Tuning of this parameter is a bit more difficult. It involves changing V_{Na}. This can be tuned by a combination of raising or lowering V_{sat}, V_{amp} (which in our case was tied to V_{dd}), $V_{\tau m}$, or $V_{\tau h}$. However, notice that moving any of these values causes a change in the time constants. Therefore, care must be taken
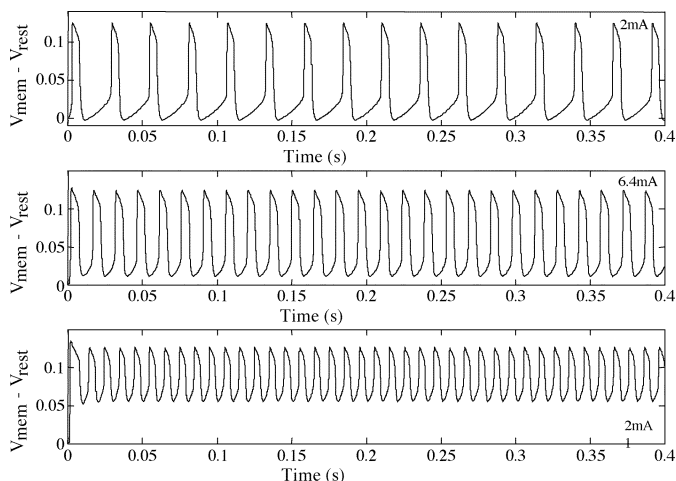
Fig. 13. Using the EKV model, the circuit can be accurately simulated. Spike frequency change for different input currents (2 μA, 6.4 μA, and 21 μA respectively) can clearly be seen.

not to tune the parameters out of the desired range when tuning this part of the circuit.

In the case of the whole neuron circuit, voltage clamp experiments are not particularly useful. A current clamp experiment, however, will allow us to see an action potential. For this type of experiment, a known current is injected onto the node, and the voltage response is observed. For low amplitudes of input current, an action potential is not generated. A depolarization can be observed, but the voltage never reaches the threshold voltage where the Na$^+$ channel fully activates. However, once a large enough current is injected, action potentials are generated and can be observed as in Fig. 12(b). Currents in the particular channels during the action potential are shown in Fig. 12(c) and (d).

It is worth noting here that all of the currents seen here are quite high compared to biological channels and neurons. This is due to the fact that the devices used in this system had W/L ratios of near 1500. They are, however, on chip fabricated with a 0.5-μm process available through MOSIS. Capacitors were discrete, so they were much larger than biology and the sizes that would be used on chip. Simulation results with more reasonable W/L ratios ($W/L = 2$) and capacitor sizes ($\sim$100's fF), as well as experimental results, have also shown that the concept works for smaller circuits.

We also simulated this circuit in SPICE using Enz–Krumme-nacher–Vittoz (EKV) models [13]. Since this circuit is running in the subthreshold regime, common models such as BSIM can not be used to accurately predict experimental measurements. Using the EKV model, simulation results closely matched experimental measurements. Simulation data for several different input currents is shown in Fig. 13. Simulation parameters are shown in Table I. Notice that the spikes look very similar from one to the next, save that the approach to the threshold voltage is much faster. The spikes in the third graph have decreased in size, but the input current is 21 μA which is huge for this circuit, and has a good chance of killing a real cell. An input of this size causes a significant change on charge stored on C_{mem} causing an increase in the resting potential.

TABLE I
BIAS VALUES FOR ONE PARTICULAR SIMULATION PARADIGM. NOTICE THAT THE DIFFERENCE BETWEEN E_{Na} AND E_{K} IS 150 mV

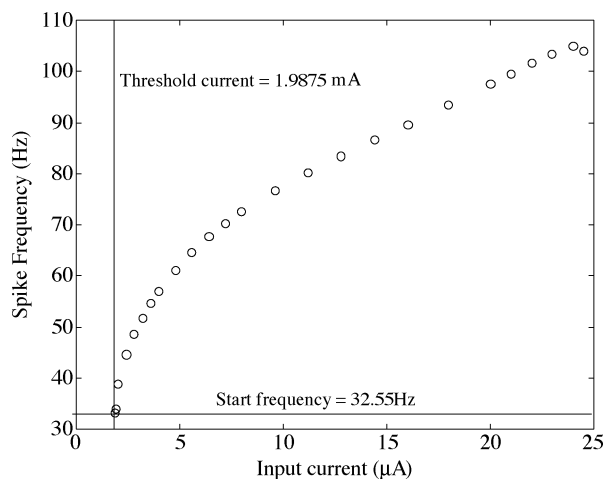| Node Name	Voltage (V)
$V_{\tau h}$	0.276
$V_{\tau m}$	1.01
V_{amp}	1.13
V_{sat}	0.325
E_{Na}	0.975
E_{K}	0.825
V_{gk}	0.322
$V_{\tau n}$	-0.31

Fig. 14. Frequency versus current for EKV model simulation of complete neuron model. The result is consistent with Hodgkin and Huxley type neurons.

Due to the fact that this circuit can be tuned to operate in many different regions, certain action potentials can look quite different from each other. However, for a fixed set of biases, the action potentials will look very similar to each other regardless of the magnitude of the input current with only the frequency of action potentials changing. The dynamics of the action potential are not affected (for reasonable current magnitudes) since the control circuitry of both channels is current isolated due to the capacitors. If the voltage on V_{mem} never changes, the current through the channel transistors will also not change. The size of the input current builds up charge on C_{mem} (and therefore voltage on V_{mem}) with a rate that is in proportion to the magnitude of that input current. Higher current means faster charge rate, which means that V_{mem} reaches threshold voltage that much quicker.

A frequency versus current plot can be seen in Fig. 14. The shape as well as the frequencies correspond well to data from real neurons [4, Fig. 4d]. This is simulated data. Real data of this type proved to be quite problematic to attain due to high-frequency ambient noise, and instrument difficulties. As illustrated in Fig. 15, high-frequency components will pass through the Na$^+$ amplifier and cause an action potential. The experiment here shows the neuron circuit response to a large hyperpolarizing input that is suddenly released. It causes an action potential to be generated. This result is expected from the biology and is referred to as a postinhibitory rebound. For an example, see [14].
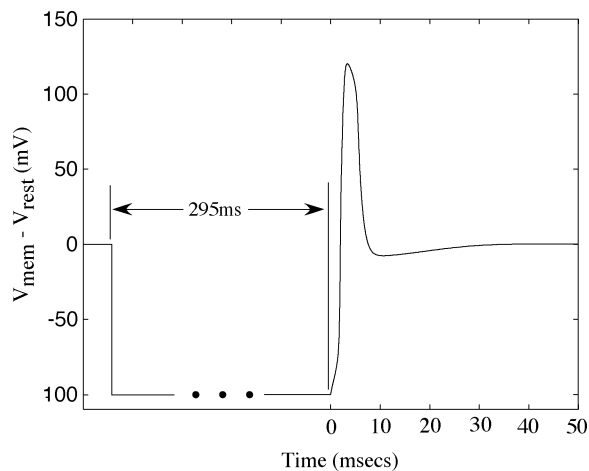
Fig. 15. Response of the Na$^+$ circuit to a large hyperpolarizing event. An action potential is generated after the release of the hyperpolarizing event. This response is consistent with biology and is referred to a postinhibitory rebound.
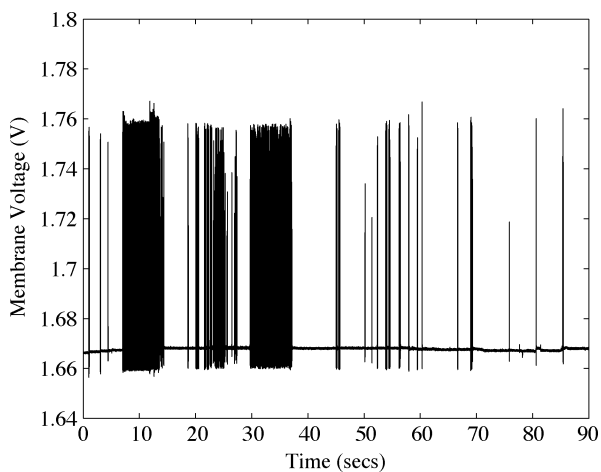
Fig. 16. Experimental measurements of the neuron circuit with the input current biased just below the threshold of firing. The activity seen is in response to ambient noise. This noise adds to the input current signal to push the circuit past the threshold voltage and cause firing to occur.

During the frequency versus current test, a particular current would be input which theoretically should cause a steady firing frequency. However, high-frequency ambient noise sources would cause the spike frequency from one sample frame to the next to change significantly. Therefore a reliable data set was not aquired.

As a final illustration of this point, look at the real data shown in Fig. 16. A constant, below spiking threshold current was placed on the membrane node. The aforementioned high-frequency ambient noise sources cause the circuit to spike randomly (with 0 input current, the currents generated by the noise sources are not large enough to generate spikes). This data, shown in Fig. 16, was taken over a period of 90 s. This is not meant to be a rigorous noise characterization of the chip. Rather it illustrates the difficulty in aquiring the actual frequency versus current curves.

IV. CONCLUSION

We have shown a new circuit model which accurately models action potentials and channel currents of real neurons. It generates this waveform by taking advantage of the numerous physical similarities between biological channels and silicon channels.

As with any circuit, there are some considerations to think about when using this circuit. Since these time constants are slow compared to the normal time constants in silicon technology, there is a trade off between low current levels (in the bias circuitry) and large capacitors. This is not limiting though. The size of the capacitors can be large enough without being overly huge ($\sim$100's fF) and still have current levels large enough to be accurately measured. We hope to one day fit thousands of these channel models on a single chip to approximate a coritcal cell (obviously other circuits will be involved including synapse models, dendrite models, and even other channels). Therefore, we need to optimize for space. Already more than 100 of these circuits have been placed on a chip 1.5 mm $\times$ 1.5 mm in a 0.5-μm process. As processes get smaller, and die sizes larger, thousands of models on a single die is not an unattainable goal.

There are five main biases for this circuit (excluding E_{Na} and E_K). E_{Na} and E_K should be global variables regardless of the number of channels models on chip. However, due to mismatch, presumably the other biases should not be global. Some method of generating these biases or storing them on chip needs to be investigated to achieve the density spoken of above, as pin limitations will quickly become apparent.

Several benefits arise, though, from the use of this model over other models. First, it does not attempt to model a set of equations. Recall that equations such as Hodgkin and Huxely's are curve fits to their data, and therefore, attempts to model these equations adds yet another layer of abstraction. Second, the model preserves many of the nonlinearities present in the real neuron by utilizing the same fundamental forces that move ions through a channel. Lastly, this model is very small and compact allowing for large numbers of them to be placed on chip.

ACKNOWLEDGMENT

REFERENCES

[1] A. L. Hodgkin and A. F. Huxley, "A quantitative description of membrane current and its application to conduction and excitation in nerve," *J. Physiol.*, vol. 117, pp. 500–544, 1952.
[2] E. R. Kandel, J. H. Schwartz, and T. M. Jessell, Eds., *Principles of Neural Science*. New York: McGraw-Hill, 2000.
[3] J. R. Clay, "Excitability of the squid giant axon revisited," *J. Neurophysiol.*, vol. 80, no. 2, pp. 903–913, Aug. 1998.
[4] M. Mahowald and R. Douglas, "A silicon neuron," *Nature*, vol. 345, no. 19, pp. 515–518, 1991.
[5] M. F. Simoni and S. P. DeWeerth, "Adaptation in an aVLSI model of a neuron," in *Proc. IEEE Int. Symp. Circuits Syst. (ISCAS '98)*, vol. 3, May-Jun. 1998, pp. 111–114.
[6] L. Abbott and G. LeMasson, "Analysis of neuron models with dynamically regulated conducatnaces," *Neur. Comput.*, vol. 5, no. 6, pp. 823–843, 1993.
[7] A. L. Hodgkin, *The Conduction of the Nerve Impluse*. Liverpool, U.K.: Liverpool Univ. Press, 1964.

[8] A. G. Andreou, "On physical models of neural computation and their analog VLSI implementation," *Proc. Phys. Comput.*, pp. 255–264, 1994.

[9] C. Mead, *Analog VLSI and Neural Systems*. Reading, MA: Addison-Wesley, 1989.

[10] J. Georgiou, E. M. Drakakis, C. Toumazou, and P. Premanoj, "An analogue micropower log-domain silicon circuit for the Hodgkin and Huxley nerve axon," in *Proc. IEEE Int. Symp. Circuits Syst. (ISCAS '99)*, vol. 2, May-Jun. 1999, pp. 286–289.

[11] Z. Liu, J. Golowasch, E. Marder, and L. F. Abbott, "A model neuron with activity-dependent conductances regulated by multiple calcium sensors," *J. Neurosci.*, vol. 18, no. 7, pp. 2309–2320, 1998.

[12] D. Johnston and S. Wu, *Foundations of Cellular Neurophysiology*. Cambridge, MA: MIT Press, 1999.

[13] C. Enz, F. Krummenacher, and E. Vittoz, "An analytical MOS transistor model valid in all regions of operation and dedicated to low-voltage and low-current applications," *J. Analog Integr. Circuits Signal Process.*, pp. 83–114, 1995.

[14] S. Bertrand and J. R. Cazalets, "Postinhibitory rebound during locomotor-like activity in neonatal rat motoneurons in vitro," *J. Neurophysiol.*, vol. 79, no. 1, pp. 342–351, 1998.

Ethan Farquhar (S'99) received the B.A. degree in natural science from Covenant College, Lookout Mountain, TN, the B.S. degree in computer engineering from Clemson University, Clemson, SC, in and the M.S. degree in electrical engineering from the Georgia Institute of Technology, Atlanta, 1999, 1999, and 2003, respectivley. He is currently working toward the Ph.D. degree in electrical engineering at the Georgia Institute of Technology.

He is working on modeling complex neuron structures in analog very large-scale integration technology.

Paul Hasler (S'87–A'97–M'01–SM'03) received B.S.E. and the M.S. degrees in electrical engineering from Arizona State University in 1991, and the Ph.D. degree in computation and neural systems from California Institute of Technology, Pasadena, in 1997.

He is an Associate Professor in the School of Electrical and Computer Engineering,t Georgia Institute of Technology, Atlanta. His current research interests include low power electronics, mixed-signal system integrated circuits, floating-gate MOS transistors, adaptive information processing systems, "smart" interfaces for sensors, cooperative analog-digital signal processing, device physics related to submicron devices or floating-gate devices, and analog very large-scale integration models of on-chip learning and sensory processing in neurobiology.

Dr. Hasler received the Paul Raphorst Best Paper Award, IEEE Electron Devices Society in 1997, the National Science Foundation CAREER Award and the Best Paper Award at SCI in 2001, and the Office of Naval Research YIP award in 2002.